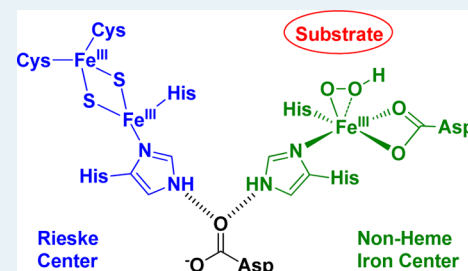


Mechanism and Catalytic Diversity of Rieske Non-Heme Iron-Dependent Oxygenases

Sarah M. Barry[†] and Gregory L. Challis^{*}

Department of Chemistry, University of Warwick, Coventry CV4 7AL, United Kingdom

ABSTRACT: Rieske non-heme iron-dependent oxygenases are important enzymes that catalyze a wide variety of reactions in the biodegradation of xenobiotics and biosynthesis of bioactive natural products. In this Perspective, we summarize recent efforts to elucidate the catalytic mechanisms of Rieske oxygenases and highlight the diverse range of reactions now known to be catalyzed by such enzymes.



KEYWORDS: dihydroxylation, C–H functionalization, amine oxidation, oxidative cyclisation, biosynthesis, biodegradation

INTRODUCTION

Selective oxidation is an important topic in the field of catalysis. Much work has focused on the discovery of catalysts able to mediate a wide variety of regio- and stereospecific oxidations on a broad range of substrates.¹ Although recent decades have heralded several important breakthroughs, the struggle to increase the enantioselectivity, regioselectivity, and catalytic efficiency of anthropogenic catalysts continues. Moreover, man-made catalysts for many types of transformation are yet to be developed, and existing catalysts are often based on heavy metals, such as osmium, ruthenium, and platinum, which are neither cost-effective nor environmentally benign.^{2,3}

In contrast, metalloenzymes such as cytochromes P450 and non-heme iron-dependent oxygenases have been shown to catalyze an array of extremely challenging oxidative transformations with a high degree of selectivity and catalytic efficiency.^{4,5} Many of these transformations are currently impossible with abiotic catalysts. The discovery and mechanistic investigation of such enzymes is thus a key component of contemporary catalysis research because they offer the potential to be developed into efficient, selective, and “green” catalysts and serve as inspiration for the development of abiotic catalysts based on inexpensive and environmentally friendly metals; for example, iron, manganese, and copper.^{6–8}

Cytochromes P450 have been studied extensively since the 1950s, and much is known about their catalytic cycles.⁵ In contrast, non-heme iron-dependent oxidative enzymes, which catalyze a wide range of reactions, including hydroxylations, oxidative cyclizations, dealkylations, desaturations, chlorinations, and epoxidations, on an array of intermediates in both catabolic and biosynthetic pathways are less well understood.^{4,9} The term “non-heme iron-dependent oxidative enzyme” encompasses several diverse enzyme families that are categorized on the basis of their substrate specificity and cofactor requirements. These families include catechol dioxygenases, lipoyxygenases, α -ketoglutarate-dependent oxy-

genases, carotenoid cleavage dioxygenases, and Rieske oxygenases.^{4,10}

Rieske oxygenases were first identified as enzymes involved in the degradation of aromatic compounds by *Pseudomonas putida*.^{11,12} These enzymes were ultimately characterized as the three component systems naphthalene dioxygenase and toluene dioxygenase.^{13–15} Today, such enzymes are best known as catalysts of the first step in the oxidative degradation of aromatic compounds via regio- and stereospecific cis-dihydroxylation to produce dihydrodiols.¹⁶ Potential applications of Rieske oxygenases in both the removal of persistent and toxic aromatic compounds from the environment and asymmetric synthesis have stimulated sustained interest.^{8,17} Moreover, it is clear from recent discoveries that the biological role of Rieske oxygenases extends far beyond the degradation of aromatic compounds. They are now known to catalyze a wide variety of oxidative transformations in a range of catabolic and biosynthetic pathways.

Several comprehensive reviews have focused on non-heme, iron-dependent oxidative enzymes in general, as well as on Rieske oxygenases specifically.^{4,10,17–19} Here, we focus on recent progress in elucidating the catalytic mechanisms of Rieske oxygenases, including insights from new model complexes and bioinspired synthetic catalysts. In addition, we describe several recently discovered Rieske oxygenases that have been reported to catalyze novel transformations. First, we summarize the state of knowledge about naphthalene dioxygenase, arguably the best-characterized Rieske oxygenase, with the intention of introducing the unfamiliar reader to this fascinating class of enzymes.

Naphthalene Dioxygenase. Dioxygenases are oxidative enzymes that catalyze the incorporation of both atoms of

Received: February 1, 2013

Revised: August 20, 2013

Published: August 28, 2013

molecular oxygen into their products. Naphthalene dioxygenase (NDO) catalyzes the *cis*-1,2-dihydroxylation of naphthalene, utilizing molecular oxygen and NADH as cosubstrates (Figure 1). Electrons from NADH are transferred to a Rieske [2Fe–2S]

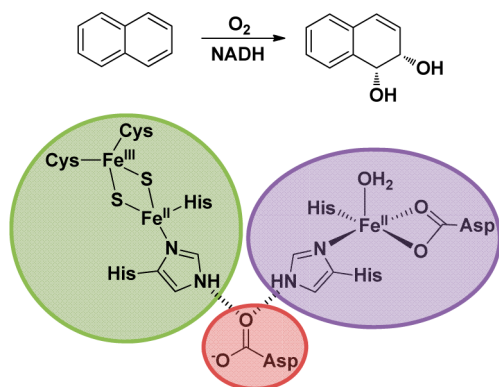


Figure 1. Reaction catalyzed by naphthalene dioxygenase (top) and architecture of the [2Fe–2S] (green) and non-heme iron (purple) centers within the α -subunits of the enzyme suggested by X-ray crystallographic analysis. A conserved aspartate residue (red) serves as a bridge between the (presumably reduced) [2Fe–2S] center and the non-heme iron center in adjacent α -subunits within the $\alpha_3\beta_3$ enzyme complex.

cluster within NDO, typically via a flavin-dependent ferredoxin reductase and a separate ferredoxin. These electrons are donated to the non-heme iron center within the active site of

the enzyme during its catalytic cycle and are used for dioxygen reduction (Figure 2).^{18,19}

The structure of naphthalene dioxygenase consists of a catalytic α -subunit and a structural β -subunit organized into an $\alpha_3\beta_3$ complex.^{19–21} The [2Fe–2S] cluster within the N-terminal Rieske domain of the α -subunit is anchored to the protein by two histidine residues and two cysteine residues within the conserved sequence motif CXHX₁₇CX₂H (Figure 1). Like many non-heme iron-dependent enzymes, the active site iron atom, which resides within the C-terminal domain, is coordinated by a so-called “2-His-1-carboxylate triad” (two histidine residues and an aspartate/glutamate residue) (Figure 1). Unlike most other enzymes belonging to this class, the carboxylate residue appears to be a bidentate ligand; however, this mode of coordination is probably flexible and is likely to be functionally inconsequential. One or two water molecules complete the coordination sphere of the iron atom.^{20,22}

The distance between the [2Fe–2S] and non-heme iron centers in adjacent α -subunits of naphthalene dioxygenase is ~ 12 Å, whereas the distance between these centers within each α -subunit is ~ 44 Å. This suggests that electron transfer between α -subunits is likely to predominate over intrasubunit electron transfer. A conserved aspartate residue bridges the [2Fe–2S] and non-heme iron centers in adjacent α -subunits via hydrogen bonds to His residues within the respective coordination spheres (Figure 1). This aspartate residue has been proposed to mediate electron transfer during the catalytic cycle.²³ In 2-oxoquinoline 8-monoxygenase from *P. putida*, the corresponding His residue within the [2Fe–2S] center is proposed to be deprotonated when the iron–sulfur cluster is in

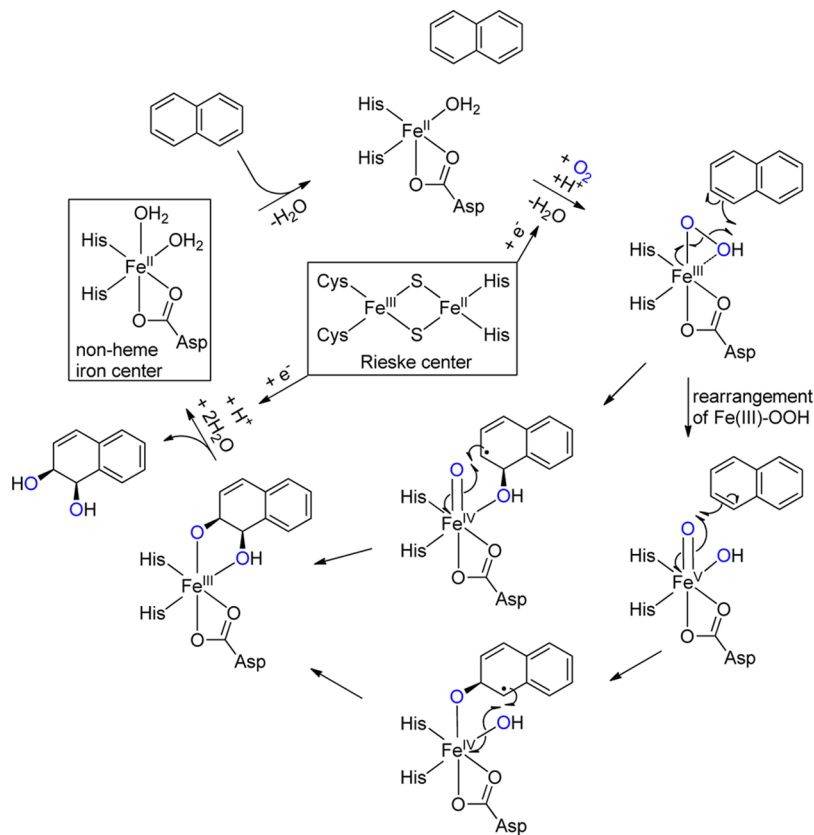


Figure 2. Proposed catalytic mechanisms for naphthalene dioxygenase. The question of whether the Fe(III)–OOH complex reacts directly with the substrate or whether it first undergoes rearrangement to an Fe(V)=O(OH) complex remains unresolved.

the oxidized form. Reduction of the iron–sulfur cluster leads to protonation of the His residue, which allows it to act as a hydrogen bond donor for the bridging aspartate. This hypothesis accounts for the conformational change observed upon reduction of the iron–sulfur cluster in 2-oxoquinoline 8-monooxygenase. One electron reduction of the Rieske cluster results in movement of the bridging aspartate toward the His residue and modification of the coordination geometry at the non-heme iron center, which is proposed to promote dioxygen binding.²⁴ In support of this hypothesis, evidence from NMR spectroscopy for reduction-coupled protonation of a histidine ligand of a [2Fe–2S] cluster in a Rieske protein within a cytochrome *bc* complex has been recently reported.²⁵ The problems associated with the paramagnetism of the Rieske cluster in these NMR experiments were overcome by selectively ¹⁵N-labeling a histidine–leucine pair.²⁵

The study of Rieske oxygenases is hampered by the oxygen-sensitivity of the [2Fe–2S] cluster. Moreover, the nature of the non-heme iron center, which lacks a significant chromophore (in contrast to cytochromes P450) and contains an EPR-silent ferrous (d⁶) iron atom in the resting state, has hindered spectroscopic studies. As a consequence, investigations using EXAFS, XANES, ENDOR, and EPR spectroscopy have largely focused on the [2Fe–2S] centers of these enzymes, whereas indirect methods, such as the generation of nitrosyl complexes and metal substitution, have typically been used to study the non-heme iron center.^{10,26,27}

Direct characterization of the non-heme iron center of naphthalene dioxygenase using NIR-MCD spectroscopy has recently been reported by Solomon and co-workers.²⁷ Such methodology has been used to study EPR-silent ferrous centers in other types of non-heme, iron-dependent enzymes.^{28–30} Using this technique, the ligand field splitting energy of the metal d orbitals can be inferred, thus facilitating assignment of the coordination geometry of the ferrous ion. In the case of naphthalene dioxygenase, the contribution of the [2Fe–2S] center to the spectrum of the *holo*-protein can be removed by subtracting the spectrum of the *apo*-protein (containing the [2Fe–2S] cluster, but not the active site ferrous ion). The application of NIR-MCD spectroscopy to naphthalene dioxygenase shows that the resting state of the non-heme iron center has a distorted octahedral geometry, regardless of whether the [2Fe–2S] center is oxidized or reduced.²⁷

Binding of naphthalene to the active site of the enzyme results in a change of the ferrous ion coordination geometry to a five-coordinate square pyramid. Reduction of the [2Fe–2S] center in this enzyme–substrate complex affords a mixture of square pyramidal (as above) and trigonal bipyramidal coordination geometries for the active site ferrous ion. Presumably, this arises from a change in protein conformation, which alters the position of the coordinating ligands and the ferrous ion, creating sufficient space in the active site for dioxygen to bind. Thus, the enzyme appears to employ an ordered mechanism in which dioxygen binds to the active site ferrous ion only after naphthalene is bound and the [2Fe–2S] center has been reduced.²⁷ Such an ordered mechanism would prevent the activation of dioxygen in the absence of naphthalene, an event that would likely lead to oxidative inactivation of the enzyme. The observation of a mixture of ferrous ion coordination geometries in the reduced enzyme–substrate complex may help to explain why extraneous active site electron density that cannot be modeled is observed in the X-ray crystal structures of several Rieske oxygenases.^{31,32}

Naphthalene dioxygenase is known to be capable of catalyzing monooxygenation reactions with substrate analogues. Lipscomb and co-workers have studied such monooxygenation reactions using cyclopropane-containing substrate analogues designed as mechanistic probes.³³ The results of these studies are inconsistent with the involvement of cationic intermediates, but are consistent with radical intermediates.³³

Despite considerable recent insight from structural, spectroscopic, and substrate analogue studies, the catalytic cycle of naphthalene dioxygenase remains to be fully elucidated. Taken together, the above data, in combination with previous mechanistic hypotheses,^{4,10,18} suggest two possible catalytic cycles for naphthalene dioxygenase in which binding of naphthalene to the active site, resulting in loss of a water ligand from the resting state octahedral ferrous complex, is a common initial step (Figure 2). Binding of oxygen to the resulting five-coordinate complex, followed by transfer of an electron from the [2Fe–2S] cluster to the non-heme center, yields a ferric peroxide complex, which undergoes protonation and loss of a water ligand to yield a bidentate hydroperoxide complex that has been observed by X-ray crystallography (Figure 2).³⁴ Coupled O–O bond cleavage and substrate oxidation yields an Fe(IV)=O complex (analogous to compound II in cytochromes P450^{5,35}) and a hydroxynaphthalene radical intermediate, which react further to yield a ferric-alkoxyhydroxynaphthalene complex (Figure 2). Alternatively, O–O bond cleavage could precede substrate oxidation, yielding a Fe(V)=O(OH) complex (analogous to compound I in the catalytic mechanism of cytochromes P450^{5,35,36}), which subsequently reacts with the substrate to form the ferric alkoxyhydroxynaphthalene complex.^{4,10,18} Transfer of a second electron from the Rieske cluster to the non-heme iron center results in formation of a ferrous alkoxyhydroxynaphthalene complex, and protonation of the alkoxide results in product release and regeneration of the resting state of the enzyme (Figure 2).

Insight into the Catalytic Mechanisms of Rieske Oxygenases from Synthetic Model Complexes. The study of synthetic complexes designed to mimic Rieske oxygenases has contributed to the development of mechanistic hypotheses for naphthalene dioxygenase and related enzymes.^{7,37} Here, we summarize some recent developments in the study of such complexes and discuss the implications of these investigations for the catalytic cycles of Rieske oxygenases.

Although the overwhelming majority of research in this area has focused on mimics of the non-heme iron catalytic center of Rieske oxygenases, it is noteworthy that a synthetic mimic of the [2Fe–2S] center in these enzymes has recently been reported (Figure 3).³⁸ The solubility of this complex in organic solvents facilitates the study of its electronic properties because

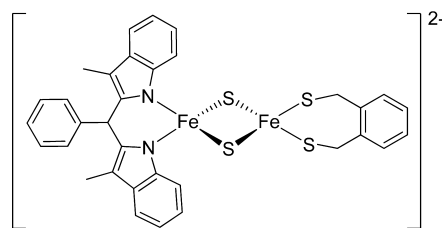


Figure 3. Structure of a synthetic complex designed to mimic the [2Fe–2S] cluster in Rieske oxygenases.

low-temperature spectroscopic techniques can be employed. EPR and Mössbauer spectroscopy have demonstrated that the model complex behaves similarly to the [2Fe–2S] cluster in the enzymes.³⁸

A key question that several researchers have attempted to address by studying synthetic mimics of the non-heme iron center is the nature of the oxidant in Rieske oxygenases. As discussed above, there are two possibilities: Fe(III)–OOH and Fe(V)=O(OH). Although it has been accepted for many years that the oxidant employed by cytochromes P450 is formally an Fe(V)=O complex (compound I), recent experimental observation of the oxidant demonstrates that it is, in fact, an Fe(IV)=O–porphyrin radical cation;³⁶ that is, the Fe(V) oxidation state is stabilized by the electron-rich porphyrin. It is not clear whether Rieske oxygenases are able to generate an Fe(V)=O(OH) intermediate because they lack a porphyrin to stabilize the Fe(V) oxidation state. Other non-heme iron-dependent oxygenases, such as those that utilize α -ketoglutarate as a source of electrons, are believed to utilize Fe(IV)=O species as active oxidants. In the case of TauD, this reactive intermediate has been observed and characterized spectroscopically.³⁹

Cho et al. recently reported the synthesis of a non-heme iron hydroperoxide complex via protonation of a bidentate peroxide complex generated from a TMC–Fe(II) complex using hydrogen peroxide (Figure 4).⁴⁰ The TMC–Fe(III)–OOH

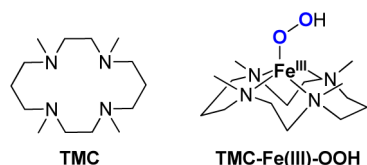


Figure 4. Structures of the TMC ligand and the TMC–Fe(III) hydroperoxide complex.

complex decays to an Fe(IV)=O complex, both of which were spectroscopically characterized using a variety of techniques. Interestingly, both the Fe(III)–OOH and Fe(IV)=O complexes are active oxidants. The ferric hydroperoxide complex is capable of acting as both a nucleophilic and an electrophilic oxidant, whereas the Fe(IV)=O species is only an electrophilic oxidant. The ferric hydroperoxide is also the more reactive oxidant. It is argued that the decay of the ferric hydroperoxide complex to the Fe(IV)=O species does not occur via an Fe(V) intermediate, in contrast to an earlier report,⁴¹ occurring instead via protonation-assisted homolysis of the ferric hydroperoxide complex.

The first non-heme Fe(V)=O complex to be fully characterized was generated from a TAML–Fe complex using *m*-CPBA⁴² (Figure 5). It was found to be stable for 1 month at 77 K and was able to oxidize thioanisole to the corresponding sulfoxide and alkenes to epoxides. However, the geometrical constraints of the ligand do not allow the formation of an

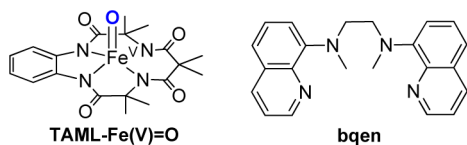


Figure 5. Structures of TAML–Fe(V)=O, the first non-heme Fe(V)=O complex to be characterized, and the BQEN ligand.

Fe(V)=O(OH) complex analogous to the proposed intermediate in the catalytic cycle of Rieske oxygenases. Subsequently, Yoon et al. reported alkene oxidation by an Fe–BQEN complex using peracetic acid as the oxidant to generate an Fe(IV)=O species⁴³ (Figure 5). However, spectroscopic data argue against the involvement of an Fe(IV)=O species as the oxidant, leading the authors to speculate that an Fe(V)=O intermediate may be involved.

Costas and co-workers recently reported the first observation of a Fe(V)=O(OH) species via VT-MS and the reactions of this complex with C–H and C=C bonds.⁴⁴ The Fe(V)=O(OH) species was found to be a reactive oxidant that is capable of *cis*-dihydroxylation of alkenes. Incorporation of labels from both H₂¹⁸O₂ and H₂¹⁸O into the products suggests that cleavage of the O–O bond in the ferric hydroperoxide complex may be assisted by a water ligand (Figure 6). This work provides the first convincing demonstration that an Fe(V)=O(OH) species can be generated and is capable of alkene dihydroxylation reactions.

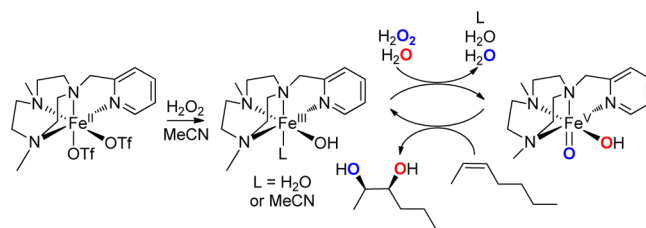


Figure 6. First example of alkene *cis*-dihydroxylation by a Fe(V)=O(OH) model complex.

Studies of model complexes have demonstrated that both Fe(III)–OOH and Fe(V)=O(OH) species can be synthesized and are capable of alkene dihydroxylation, providing support for the proposal that analogous species participate in the catalytic mechanism of naphthalene dioxygenase. A recent study of TMC- and N4Py-based model complexes by Solomon and co-workers indicates that a high-spin Fe(III)–OOH species is sufficiently electrophilic to react directly with naphthalene.⁴⁵ Thus, it is suggested that formation of an Fe(V)=O(OH) intermediate in the catalytic cycle of NDO is not necessary. Nevertheless, the question of whether a high spin Fe(III)–OOH complex or an Fe(V)=O(OH) complex is used by the enzyme as the reactive oxidant remains open.

Catalytic Diversity of Rieske Oxygenases. Although Rieske oxygenases are best known for catalyzing bacterial arene dihydroxylation reactions, it is becoming increasingly apparent that members of this enzyme family catalyze a wide variety of other transformations in diverse organisms, including bacteria, plants, insects, and mammals. A recent phylogenetic analysis of Rieske oxygenases highlights this important point by revealing that the bacterial arene-hydroxylating enzymes fall into a very small cluster within one of two main groups, and only five of them are associated with a recognizable β subunit.⁴⁶ In this section, we highlight several recently discovered examples of Rieske oxygenases that catalyze a range of transformations in catabolic and biosynthetic pathways, thus illustrating the functional diversity of this enzyme family.

Enzymes Involved in Catabolic Pathways. KshAB is a two-component Rieske oxygenase encoded by genes within a *Mycobacterium tuberculosis* gene cluster responsible for cholesterol catabolism, which may facilitate the bacterium's

survival in macrophages and may also play a role in pathogenesis.⁴⁷ Eltis and co-workers have shown that this enzyme catalyzes monohydroxylation of 4-androstene-3,17-dione (AD), and 1,4-androstadiene-3,17-dione (ADD) (Figure 7). However, consumption of oxygen appears to be faster in the

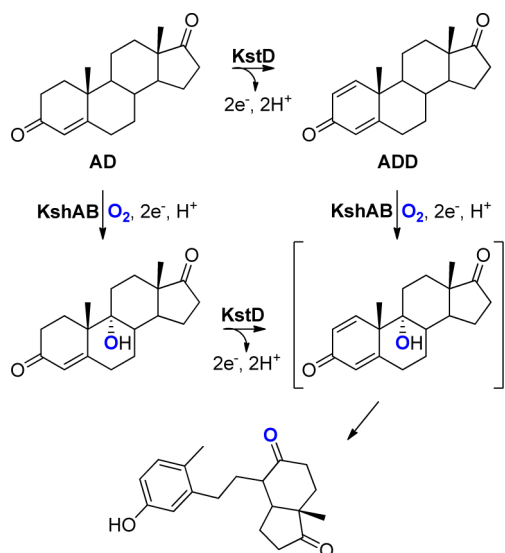


Figure 7. Hydroxylation reactions catalyzed by KshAB in *M. tuberculosis* cholesterol catabolism. AD, 4-androstene-3,17-dione; ADD, 1,4-androstadiene-3,17-dione.

presence of ADD ($K_m = 110 \pm 20 \mu M$, $V_{max} = 0.32 \pm 0.02 \mu M s^{-1}$) than AD ($K_m = 24 \pm 16 \mu M$, $V_{max} = 0.032 \pm 0.006 \mu M s^{-1}$).³¹ Both of these KshAB-catalyzed reactions are relatively slow, suggesting that an additional factor may increase the catalytic efficiency of the enzyme in vivo or that a different intermediate in cholesterol catabolism is the true substrate of the enzyme. KshA has low sequence identity ($\sim 11\%$) to the α -subunits of well-characterized Rieske oxygenases, for example, phthalate dioxygenase from *Burkholderia cepacia*, 2-oxoquinoline 8-monoxygenase from *P. putida*, and cardo13 from *Janthinobacterium* sp., suggesting it belongs to a distinct subfamily. This view is reinforced by X-ray crystallographic analysis, which shows that although KshA contains a $[2Fe-2S]$ cluster and a non-heme center, it lacks several other typical features of Rieske oxygenases.³¹ The nature of one of the nonprotein ligands of the non-heme iron center was not clear from this analysis, leading the authors to suggest that a mixture of species with multiple occupancies is present. Identification of the substrate binding site in KshA via docking studies may pave the way for the design of inhibitors, which could serve as leads for the development of novel drugs to treat tuberculosis. Inhibitors that cause uncoupling of oxygen activation and substrate oxidation would be of particular interest, because they could both inhibit cholesterol catabolism and lead to the production of damaging reactive oxygen species in *M. tuberculosis*.³¹

Another cholesterol-metabolizing Rieske oxygenase has recently been reported by Niwa and co-workers.⁴⁸ The DAF-36/neverland gene is conserved in nematodes and insects and its deletion is lethal. In vitro assays suggest that the corresponding enzyme catalyzes the conversion of cholesterol to 7,8-dehydrocholesterol, possibly via a monohydroxylated species that undergoes subsequent dehydration, although direct desaturation cannot be excluded (Figure 8). However, the

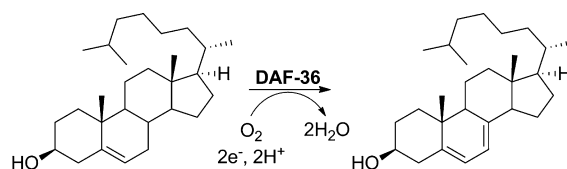


Figure 8. Desaturation of cholesterol catalyzed by DAF-36 in vitro. The essential role for survival of nematodes and insects played by DAF-36 in vivo is unclear.

biological relevance of this reaction is not clear. Although it is postulated that this enzyme is involved in cholesterol homeostasis, further studies will be required to determine the true function of this essential enzyme in vivo.⁴⁸

Dicamba O-demethylase catalyzes the oxidative O-demethylation of the broadleaf herbicide dicamba as the first step of its degradation in plants (Figure 9). The product of this reaction is

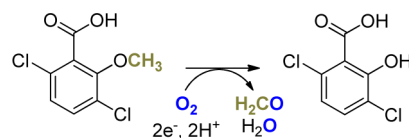


Figure 9. O-Demethylation reaction catalyzed by dicamba O-demethylase, the first step in the degradation of the herbicide dicamba in plants.

no longer herbicidal. Thus, the gene encoding dicamba O-demethylase may prove useful in the development of genetically modified crops that are resistant to dicamba. As for KshA, there is low sequence similarity ($\sim 18\%$) between dicamba O-demethylase and structurally characterized homologues. The X-ray crystal structure of this enzyme, the first for a Rieske oxygenase that catalyzes exocyclic monooxygenation, was recently reported, reinforcing the conformational flexibility and frequently ambiguous nature of the nonprotein ligands of the non-heme iron center in enzymes belonging to this enzyme family.³² One interesting feature of dicamba O-demethylase revealed by the structural analysis is the presence of an asparagine residue in the vicinity of the non-heme iron center. Although the amido group of this residue is too far away from the iron atom (3.5 Å) in the crystal to act directly as a ligand, it is tempting to speculate that in solution, a conformational change allows the Asn residue to coordinate the ferrous ion. A similar coordination of the active site ferrous ion by the amido side chain of Gln has been observed for the resting state of isopenicillin N synthase (IPNS), an enzyme belonging to the α -ketoglutarate-dependent non-heme iron oxygenase superfamily (note that unlike other members of this family, IPNS does not require α -ketoglutarate as a cosubstrate).^{49–51} Substrate binding to IPNS results in displacement of the Gln ligand, which allows subsequent binding of dioxygen to the active site ferrous ion.

Several bacteria are able to utilize caffeine as a sole source of carbon and have thus developed a variety of pathways for caffeine degradation. Subramanian and co-workers recently reported the characterization of NdmA and NdmB, two Rieske oxygenases from *P. putida* CBBS that are able to catalyze the oxidative N_1 -demethylation and N_3 -demethylation, respectively, of caffeine, as well as several methylated xanthine derivatives.⁵² On the basis of the substrate preferences of the enzymes, it was proposed that NdmA and NdmB act sequentially in the demethylation of caffeine (Figure 10).⁵² NdmD was identified

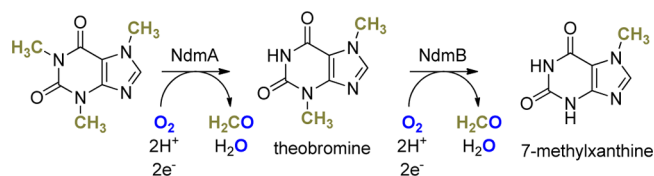


Figure 10. Degradation of caffeine catalyzed by NdmA and NdmB to form 7-methylxanthine. Electrons are supplied to NdmA and NdmB by the NADH-dependent reductase NdmD.

as a NADH-dependent reductase able to supply electrons to the [2Fe–2S] centers of NdmA and NdmB. This pathway is similar to the cytochrome P450-mediated caffeine degradation pathway in humans.^{53,54}

Enzymes involved in biosynthetic pathways. Pyrrolnitrin, a broad spectrum antifungal, is produced by several *Pseudomonas* and *Burkholderia* species.^{55–57} In 2005, Zhao and co-workers reported the biochemical characterization of PrnD, a novel Rieske oxygenase that catalyzes the oxidation of an aniline derivative to the corresponding nitrobenzene derivative in pyrrolnitrin biosynthesis (Figure 11).⁵⁸ Analogous oxidation

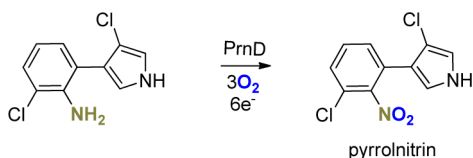


Figure 11. Reaction catalyzed by PrnD in pyrrolnitrin biosynthesis.

reactions in other biosynthetic pathways have been shown to be catalyzed by cytochromes P450 and non-heme diiron-dependent oxygenases.^{5,59} PrnD is the first example of a Rieske oxygenase with the ability to catalyze this type of transformation.

Subsequently, PrnD was shown to catalyze the oxidation of other arylamines to the corresponding nitroarenes;^{60,61} however, these transformations are less efficient, and only a limited range of substrate analogues is tolerated. Investigation of the PrnD-catalyzed oxidation of 4-aminobenzylamine to 4-nitrobenzylamine showed that the reaction proceeds via sequential oxidation of the amino group.^{60,61} The hydroxylamine is an isolatable intermediate that undergoes dehydrogenation to generate the nitrosoarene, which is further oxidized to the nitroarene. On the basis of mutagenesis studies and the intermediates accumulated, it is proposed that the rate-limiting reaction in the overall transformation is dehydrogenation of the hydroxylamine.^{60,61} Both atoms of the nitro group are labeled when the PrnD-catalyzed oxidation of 4-aminobenzylamine is carried out under an ¹⁸O₂ atmosphere, whereas no labeling of the nitrosoarene intermediate was observed when the PrnD-catalyzed oxidation of the unlabeled hydroxylamine intermediate was carried out under an ¹⁸O₂ atmosphere (Figure 12). This

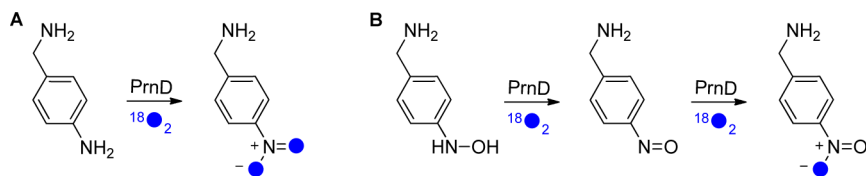


Figure 12. Incorporation of labeled dioxygen into intermediates and/or the product during PrnD-catalyzed oxidation of 4-aminobenzylamine (A) and 4-hydroxylaminobenzylamine (B).

led the authors to propose that the conversion of the hydroxylamine to the nitrosoarene involves direct dehydrogenation rather than proceeding via a dihydroxylated amine intermediate. However, if the dihydroxylated amine intermediate were to remain enzyme-bound, it is conceivable that dehydration of the intermediate could proceed via exclusive loss of the ¹⁸O-labeled hydroxyl group.

Streptorubin B and metacycloprodigiosin are antipodal members of the prodiginine alkaloid family of antimalarial natural products produced by *Streptomyces coelicolor* M145 and *Streptomyces longisporus* DSM40667, respectively.^{62–64} (Figure 13). They can be envisioned to arise from the common precursor undecylprodigiosin via regio- and stereodivergent oxidative carbocyclization reactions (Figure 13). The *redG* gene, which is embedded within a cluster of genes responsible for the assembly of streptorubin B and undecylprodigiosin in *S. coelicolor*, encodes a protein with sequence similarity to Rieske oxygenases, such as naphthalene dioxygenase.^{65–68} Indeed, a sequence alignment with the naphthalene dioxygenase α -subunit reveals that the N-terminal domain of RedG contains the His and Cys residues that bind the [2Fe–2S] cluster and the C-terminal domain contains the two His residues of the 2-His-1-carboxylate iron-binding triad in the non-heme center (there are several candidates in RedG for the carboxylate residue of the triad).⁶⁸ Interestingly, the “bridging” aspartate residue implicated in electron transfer from the [2Fe–2S] center to the non-heme iron center in naphthalene dioxygenase appears to be mutated to glutamate in RedG.⁶⁸ Deletion of *redG* in *S. coelicolor* abrogates the production of streptorubin B, but not undecylprodigiosin, and undecylprodigiosin is converted to streptorubin B upon feeding to heterologous *Streptomyces* hosts that have been engineered to express *redG*.^{68,69} This demonstrates that *redG* catalyzes the oxidative carbocyclization of undecylprodigiosin to form streptorubin B (Figure 13). The *mcpG* gene, which encodes a *redG* orthologue, was cloned from *S. longisporus* and sequenced.⁶⁸ Expression of *mcpG* in the *redG* mutant of *S. coelicolor* resulted in exclusive production of metacycloprodigiosin, demonstrating that *McpG* catalyzes the conversion of undecylprodigiosin to metacycloprodigiosin (Figure 13).

The oxidative carbocyclization reactions catalyzed by RedG and *McpG* are unprecedented transformations for Rieske oxygenases. Indeed, all known oxidative cyclization reactions catalyzed by non-heme iron and oxygen-dependent enzymes result in the formation of heterocycles. By analogy with naphthalene dioxygenase, we propose a catalytic mechanism for RedG involving initial binding of undecylprodigiosin to the active site, resulting in loss of a water ligand from the resting state octahedral ferrous complex (Figure 14). Oxygen binding and transfer of an electron from the [2Fe–2S] cluster to the non-heme center results in formation of a peroxide complex that undergoes protonation and loss of a water ligand to form a bidentate ferric hydroperoxide complex, as observed for

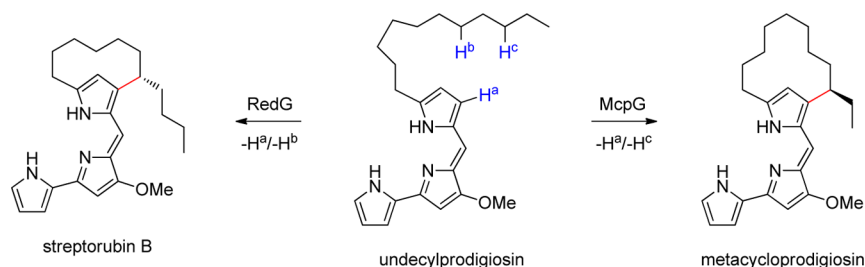


Figure 13. Regio- and stereodivergent oxidative carbocyclization reactions catalyzed by the Rieske oxygenase-like enzymes RedG and McpG in streptorubin B and metacycloprodigiosin biosynthesis, respectively.

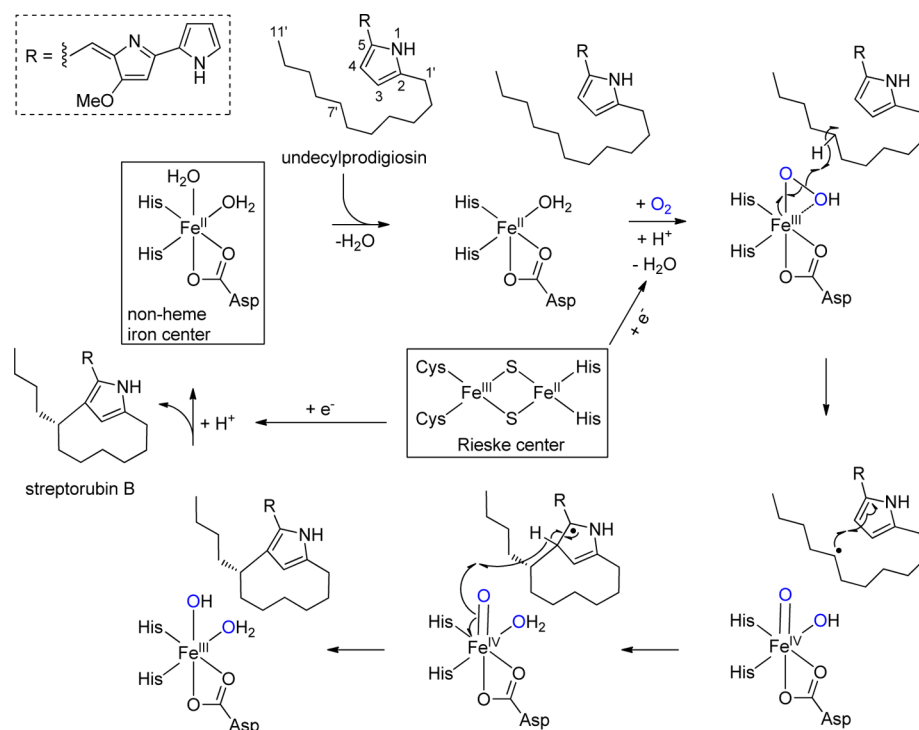


Figure 14. Proposed catalytic mechanisms for the *redG*-catalyzed oxidative carbocyclization of undecylprodigiosin to form streptorubin B. As for naphthalene dioxygenase, it is unclear whether the Fe(III)–OOH complex reacts directly with the substrate or undergoes rearrangement to an Fe(V)=O(OH) complex prior to reacting.

naphthalene dioxygenase (Figure 14). O–O bond cleavage coupled with abstraction of a hydrogen atom from the C-7' of undecylprodigiosin yields a Fe(IV)=O(OH₂) complex and a secondary alkyl radical (Figure 14). Alternatively, this may occur in two steps, in which O–O bond cleavage yields a Fe(V)=O(OH) complex that subsequently abstracts a hydrogen atom from the C-7' of the substrate. Irrespective of the timing of O–O bond cleavage relative to hydrogen atom abstraction, the resulting secondary alkyl radical can add to C-4 of the pyrrole to generate a tertiary radical that is stabilized by delocalization into the neighboring highly conjugated π -system (Figure 14). The Fe(IV)=O(OH₂) complex can then abstract a hydrogen atom from the C-4 of the pyrrole to generate streptorubin B. Transfer of a second electron from the Rieske cluster to the non-heme iron center, followed by protonation of the hydroxide ligand in the resulting Fe(II)(OH₂)(OH) complex, results in product release and regeneration of the resting state of the enzyme (Figure 14). It is important to note, however, that alternative mechanisms, for example, involving abstraction of hydride from the alkyl chain to form a

carbocation intermediate that subsequently reacts with the pyrrole, cannot be ruled out at this stage.

CONCLUSIONS

Recent studies of Rieske oxygenases, as well as biomimetic model complexes, have significantly advanced our understanding of such non-heme iron-dependent oxidation biocatalysts. Nevertheless, key questions remain. For example, although considerable recent progress has been made in the use of model complexes to delineate potential oxidizing species, the precise nature of the reactive intermediate generated by Rieske oxygenases remains to be defined and fully characterized. Moreover, the factors that affect the fate of this reactive intermediate, leading to different reaction outcomes such as dioxygenation, monooxygenation, desaturation and oxidative cyclization, remain unclear.

The genomics revolution has uncovered a wealth of novel enzymes belonging to the Rieske oxygenase family. This has greatly expanded the range of reactions known to be catalyzed by such enzymes, which may aid our understanding of how the fate of the reactive oxidizing species is controlled. However, it is

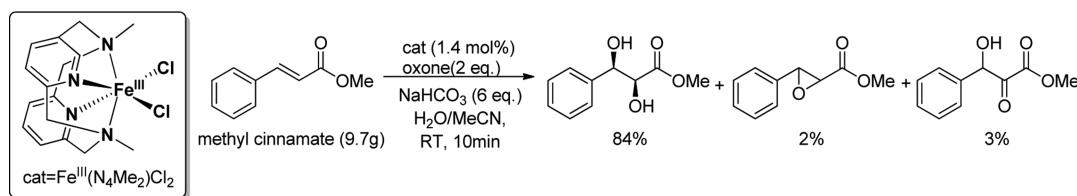


Figure 15. Large-scale cis-dihydroxylation of methyl cinnamate catalyzed by $\text{Fe}^{\text{III}}(\text{N}_4\text{Me}_2)\text{Cl}_2$. Epoxide and α -hydroxyketone byproducts are also formed in small amounts.

clear from recent studies that searches based on sequence similarity with well-characterized examples such as naphthalene dioxygenase fall short of defining the full extent of this enzyme family, as a result of the large sequence diversity among enzymes sharing the Rieske oxygenase fold.^{46,70}

A key challenge for the future is to translate fundamental work on Rieske oxygenases and their mimetics into synthetically useful catalysts. Bacteria containing Rieske oxygenases have found application in the production of homochiral starting materials for organic synthesis and in soil bioremediation via degradation of aromatic pollutants. However, direct application of the isolated enzymes presents several challenges, including the oxygen sensitivity of the $[2\text{Fe}-2\text{S}]$ cluster, enzyme instability, and the expensive NAD(P)H cosubstrate requirement.^{8,71,72}

One potential application of biomimetic complexes is alkene cis-dihydroxylation.⁷² Current synthetically useful anthropogenic catalysts for this reaction rely on toxic heavy metals such as osmium (e.g., Sharpless's asymmetric dihydroxylation catalyst). An iron-based catalyst would be less expensive and would generate less toxic waste. However, one of the problems with many current iron-based catalysts is that the substrate must be used in excess, creating issues with process scaleup. In an effort to overcome this, Che and co-workers have reported the use of a variety of iron complexes, previously reported as models for catechol dioxygenase by Krüger and co-workers,^{73,74} in conjunction with oxone (peroxymonosulphate) rather than hydrogen peroxide as the oxidant. These complexes were used to oxidize a variety of alkenes with good selectivity for the *cis*-diol and with excellent conversion on a significant scale ($\sim 10\text{g}$) (Figure 15).⁷⁴

Although there are significant hurdles to overcome, it is hoped that ongoing studies of Rieske oxygenases will ultimately aid the development of efficient, inexpensive, and environmentally friendly (bio)catalysts capable of a wide variety of oxygenation and C–H activation reactions.

AUTHOR INFORMATION

Corresponding Author

*Phone: +44 (0) 2476 574024. Fax +44 (0) 2476 524112. E-mail: g.l.challis@warwick.ac.uk.

Present Address

[†](S.M.B.) Department of Chemistry, School of Biomedical Sciences, King's College London, London SE1 1DB, U.K.

Notes

The authors declare no competing financial interest.

ACKNOWLEDGMENTS

The NIH is gratefully acknowledged for supporting research on Rieske oxygenase-like enzymes in GLC's lab (Grant 1R01GM77147-01A1).

ABBREVIATIONS:

AD,4-androstene-3,17-dione; ADD,1,4-androstadiene-3,17-dione; BQEN,*N,N'*-dimethyl-*N,N'*-bis(8-quinolyl)ethane-1,2-diamine; *m*-CPBA,*meta*-chloroperbenzoic acid; EXAFS,extended X-ray absorption fine structure; ENDOR,electron–nuclear double resonance; EPR,electron paramagnetic resonance; NADH,reduced nicotinamide adenine dinucleotide; NIR-MCD,near-infrared magnetic circular dichroism; NMR,nuclear magnetic resonance; N4Py,*N,N*-bis(2-pyridylmethyl)-*N*-bis(2-pyridyl)methylamine; Py-TACN,1-(2'-pyridylmethyl)-4,7-dimethyl-1,4,7-triazacyclonane; TMC,1,4,8,11-tetramethyl-1,4,8,11-tetraazacyclotetradecane; TAML,tetraamido macrocyclic ligand; VT-MS,variable temperature mass spectrometry; XANES,X-ray absorption near edge structure

REFERENCES

- Punniyamurthy, T.; Velusamy, S.; Iqbal, J. *Chem. Rev.* **2005**, *105*, 2329–2364.
- Trindade, A. F.; Gois, P. M. P.; Afonso, C. A. M. *Chem. Rev.* **2009**, *109*, 418–514.
- Bates, R. *Organic Synthesis Using Transition Metals*, 2nd ed.; John Wiley & Sons, Ltd: Chichester, UK, 2012.
- Costas, M.; Mehn, M. P.; Jensen, M. P.; Que, L., Jr. *Chem. Rev.* **2004**, *104*, 939–986.
- Ortiz de Montellano, P. R.; De Voss, J. J., Eds.; *Cytochrome P450: Structure, Mechanism and Biochemistry*, 3rd ed.; Springer-Verlag: New York, 2008.
- Turner, N. J. *Chem. Rev.* **2011**, *111*, 4073–4087.
- Que, L., Jr.; Tolman, W. B. *Nature* **2008**, *455*, 333–340.
- Parales, R. E.; Resnick, S. M. In *Applications of Aromatic Hydrocarbon Dioxygenases in Biocatalysis in the Pharmaceutical and Biotechnology Industries*; Patel, R. N., Ed.; CRC Press: Boca Raton, FL, 2006.
- Resnick, S. M.; Lee, K.; Gibson, D. T. *J. Ind. Microbiol. Biotechnol.* **1996**, *17*, 438–457.
- Abu-Omar, M. M.; Loaiza, A.; Hontzeas, N. *Chem. Rev.* **2005**, *105*, 2227–2252.
- Axcell, B. C.; Geary, P. J. *Biochem. J.* **1975**, *146*, 173–183.
- Gibson, D. T.; Koch, J. R.; Kallio, R. E. *Biochemistry* **1968**, *7*, 2653–2662.
- Yeh, W.-K.; Gibson, D. T.; Liu, T.-N. *Biochem. Biophys. Res. Commun.* **1977**, *78*, 401–410.
- Ensley, B. D.; Gibson, D. T. *J. Bacteriol.* **1983**, *155*, 505–511.
- Ensley, B. D.; Gibson, D. T.; Laborde, A. L. *J. Bacteriol.* **1982**, *149*, 948–954.
- Jerina, D. M.; Daly, J. W.; Jeffrey, A. M.; Gibson, D. T. *Arch. Biochem. Biophys.* **1971**, *142*, 394–396.
- Mohammadi, M.; Viger, J. F.; Kumar, P.; Barriault, D.; Bolin, J. T.; Sylvestre, M. *J. Biol. Chem.* **2011**, *286*, 27612–27621.
- Bugg, T. D. H.; Ramaswamy, S. *Curr. Opin. Chem. Biol.* **2008**, *12*, 134–140.
- Ferraro, D. J.; Gakhar, L.; Ramaswamy, S. *Biochem. Biophys. Res. Commun.* **2005**, *338*, 175–190.
- Parales, R. E. *J. Ind. Microbiol. Biotechnol.* **2003**, *30*, 271–278.
- Kauppi, B.; Lee, K.; Carredano, E.; Parales, R. E.; Gibson, D. T.; Eklund, H.; Ramaswamy, S. *Structure* **1998**, *6*, 571–586.

- (22) Koehntop, K. D.; Emerson, J. P.; Que, L., Jr. *J. Biol. Inorg. Chem.* **2005**, *10*, 87–93.
- (23) Parales, R. E.; Parales, J. V.; Gibson, D. T. *J. Bacteriol.* **1999**, *181*, 1831–1837.
- (24) Martins, B. M.; Svetlitchnaia, T.; Dobbek, H. *Structure* **2005**, *13*, 817–824.
- (25) Hsueh, K.-L.; Westler, W. M.; Markle, J. L. *J. Am. Chem. Soc.* **2010**, *132*, 7908–7918.
- (26) Kovaleva, E. G.; Neiberger, M. B.; Chakrabarty, S.; Lipscomb, J. D. *Acc. Chem. Res.* **2007**, *40*, 475–483.
- (27) Ohta, T.; Chakrabarty, S.; Lipscomb, J. D.; Solomon, E. I. *J. Am. Chem. Soc.* **2008**, *130*, 1601–1610.
- (28) Kelmsley, J. N.; Wasinger, E. C.; Datta, S.; Mitić, N.; Acharya, T.; Hedman, B.; Caradonna, J. P.; Hodgson, K. O.; Solomon, E. I. *J. Am. Chem. Soc.* **2003**, *125*, 5677–5686.
- (29) Davis, M. I.; Wasinger, E. C.; Decker, A.; Pau, M. Y. M.; Vaillancourt, F. H.; Bolin, J. T.; Eltis, L. D.; Hedman, B.; Hodgson, K. O.; Solomon, E. I. *J. Am. Chem. Soc.* **2003**, *125*, 11214–11227.
- (30) Zhou, J.; Kelly, W. L.; Bachmann, B. O.; Gunsior, M.; Townsend, C. A.; Solomon, E. I. *J. Am. Chem. Soc.* **2001**, *123*, 7388–7398.
- (31) Capyk, J. K.; D'Angelo, I.; Strynadka, N. C.; Eltis, L. D. *J. Biol. Chem.* **2009**, *284*, 9937–9946.
- (32) D'Ordine, R. L.; Rydel, T. J.; Storek, M. J.; Sturman, E. J.; Moshiri, F.; Bartlett, R. K.; Brown, G. R.; Eilers, R. J.; Dart, C.; Qi, Y.; Flasiński, S.; Franklin, S. J. *J. Mol. Biol.* **2009**, *392*, 481–497.
- (33) Chakrabarty, S.; Austin, R. N.; Deng, D.; Groves, J. T.; Lipscomb, J. D. *J. Am. Chem. Soc.* **2007**, *129*, 3514–3515.
- (34) Karlsson, A.; Parales, J. V.; Parales, R. E.; Gibson, D. T.; Eklund, H.; Ramaswamy, S. *Science* **2003**, *299*, 1039–1042.
- (35) Denisov, I. G.; Makris, T. M.; Sligar, S. G.; Schlichting, I. *Chem. Rev.* **2005**, *105*, 2253–2277.
- (36) Rittle, J.; Green, M. T. *Science* **2010**, *330*, 933–937.
- (37) Bruijninx, P. C.; van Koten, G.; Klein Gebbink, R. J. *Chem. Soc. Rev.* **2008**, *37*, 2716–2744.
- (38) Ballmann, J.; Albers, A.; Demeshko, S.; Dechert, S.; Bill, E.; Bothe, E.; Ryde, U.; Meyer, F. *Angew. Chem., Int. Ed.* **2008**, *47*, 9537–9541.
- (39) Price, J. C.; Barr, E. W.; Tirupati, B.; Bollinger, J. M., Jr.; Krebs, C. *Biochemistry* **2003**, *42*, 7497–7508.
- (40) Cho, J.; Jeon, S.; Wilson, S. A.; Liu, L. V.; Kang, E. A.; Braymer, J. J.; Lim, M. H.; Hedman, B.; Hodgson, K. O.; Valentine, J. S.; Solomon, E. I.; Nam, W. *Nature* **2011**, *478*, 502–505.
- (41) Li, F.; Meier, K. K.; Cranswick, M. A.; Chakrabarti, M.; Van Heuvelen, K. M.; Münck, E.; Que, L., Jr. *J. Am. Chem. Soc.* **2011**, *133*, 7256–7259.
- (42) de Oliveira, F. T.; Chanda, A.; Banerjee, D.; Shan, X.; Mondal, S.; Que, L.; Bominaar, E. L.; Münck, E.; Collins, T. J. *Science* **2007**, *315*, 835–838.
- (43) Yoon, J.; Wilson, S. A.; Jang, Y. K.; Seo, M. S.; Nehru, K.; Hedman, B.; Hodgson, K. O.; Bill, E.; Solomon, E. I.; Nam, W. *Angew. Chem., Int. Ed.* **2009**, *48*, 1257–1260.
- (44) Prat, I.; Mathieson, J. S.; Güell, M.; Ribas, X.; Luis, J. M.; Cronin, L.; Costas, M. *Nat. Chem.* **2011**, *3*, 788–793.
- (45) Liu, L. V.; Hong, S.; Cho, J.; Nam, W.; Solomon, E. I. *J. Am. Chem. Soc.* **2013**, *135*, 3286–3299.
- (46) Capyk, J. K.; Eltis, L. D. *J. Biol. Inorg. Chem.* **2012**, *17*, 425–436.
- (47) Van der Geize, R.; Yam, K.; Heuser, T.; Wilbrink, M. H.; Hara, H.; Anderton, M. C.; Sim, E.; Dijkhuizen, L.; Davies, J. E.; Mohn, W. W.; Eltis, L. D. *Proc. Natl. Acad. Sci.* **2007**, *104*, 1947–1952.
- (48) Yoshiyama-Yanagawa, T.; Enya, S.; Shimada-Niwa, Y.; Yaguchi, S.; Haramoto, Y.; Matsuya, T.; Shiomi, K.; Sasakura, Y.; Takahashi, S.; Asashima, M.; Kataoka, H.; Niwa, R. *J. Biol. Chem.* **2011**, *286*, 25756–25762.
- (49) Roach, P. L.; Clifton, I. C.; Hensgens, C. M. H.; Shibata, N.; Schofield, C. J.; Baldwin, J. E.; Hajdu, J. *Nature* **1997**, *387*, 827–830.
- (50) Landman, O.; Borovok, I.; Aharonowitz, Y.; Cohen, G. *FEBS Lett.* **1997**, *405*, 172–174.
- (51) Sami, M.; Brown, T.; Roach, P. L.; Baldwin, J. E.; Schofield, C. J. *FEBS Lett.* **1997**, *405*, 191–194.
- (52) Summers, R. M.; Louie, T. M.; Yu, C. L.; Gakhar, L.; Louie, K. C.; Subramanian, M. *J. Bacteriol.* **2012**, *194*, 2041–2049.
- (53) Tassaneeyakul, W.; Birkett, D. J.; McManus, M. E.; Tassaneeyakul, W.; Veronese, M. E.; Andersson, T.; Tukey, R. H.; Miners, J. O. *Biochem. Pharmacol.* **1994**, *47*, 1767–1776.
- (54) Campbell, M. E.; Grant, D. M.; Inaba, T.; Kalow, W. *Drug Metab. Dispos.* **1987**, *2*, 237–249.
- (55) Pfender, W. F.; Kraus, J.; Loper, J. E. *Phytopathology* **1993**, *83*, 1223–1228.
- (56) Schmidt, S.; Blom, J. F.; Pernthaler, J.; Berg, G.; Baldwin, A.; Mahenthiralingam, E.; Eberl, L. *Environ. Microbiol.* **2009**, *11*, 1422–1437.
- (57) Mahenthiralingam, E.; Song, L.; Sass, A.; White, J.; Wilmot, C.; Marchbank, A.; Boaisa, O.; Paine, J.; Knight, D.; Challis, G. L. *Chem. Biol.* **2011**, *18*, 665–677.
- (58) Lee, J. K.; Simurdiak, M.; Zhao, H. *J. Biol. Chem.* **2005**, *280*, 36719–36727.
- (59) Choi, Y. S.; Zhang, H.; Brunzelle, J. S.; Nair, S. K.; Zhao, H. *Proc. Natl. Acad. Sci. U.S.A.* **2008**, *105*, 6858–6863.
- (60) Lee, J.-K.; Ang, E.-L.; Zhao, H. *J. Bacteriol.* **2006**, *188*, 6179–6183.
- (61) Lee, J.; Zhao, H. *Angew. Chem., Int. Ed.* **2006**, *118*, 638–641.
- (62) Haynes, S. W.; Sydor, P. K.; Corre, C.; Song, L.; Challis, G. L. *J. Am. Chem. Soc.* **2011**, *133*, 1793–1798.
- (63) Hu, D. X.; Clift, M. D.; Lazarski, K. E.; Thomson, R. J. *J. Am. Chem. Soc.* **2011**, *133*, 1799–1804.
- (64) Papireddy, K.; Smilkstein, M.; Kelly, J. X.; Shweta, S. S. M.; Alhamadsheh, M.; Haynes, S. W.; Challis, G. L.; Reynolds, K. A. *J. Med. Chem.* **2011**, *54*, 5296–5306.
- (65) Haynes, S. W.; Sydor, P. K.; Stanley, A. E.; Song, L.; Challis, G. L. *Chem. Commun.* **2008**, *28*, 1865–1867.
- (66) Stanley, A. E.; Walton, L. J.; Kourdi Zerikly, M.; Corre, C.; Challis, G. L. *Chem. Commun.* **2006**, *14*, 3981–3983.
- (67) Cerdeño, A. M.; Bibb, M. J.; Challis, G. L. *Chem. Biol.* **2001**, *8*, 817–829.
- (68) Sydor, P. K.; Barry, S. M.; Odulate, O. M.; Barona-Gomez, F.; Haynes, S. W.; Corre, C.; Song, L.; Challis, G. L. *Nat. Chem.* **2011**, *3*, 388–392.
- (69) Sydor, P. K.; Challis, G. L. *Meth. Enzymol.* **2012**, *516*, 195–218.
- (70) Chakraborty, J.; Dutta, T. K. *J. Biomol. Struct. Dyn.* **2011**, *29*, 67–78.
- (71) van Beilen, J. B.; Duetz, W. A.; Schmid, A.; Witholt, B. *Trends Biotechnol.* **2003**, *21*, 170–177.
- (72) Nolan, L. C.; O'Connor, K. E. *Biotechnol. Lett.* **2008**, *30*, 1879–1891.
- (73) Koch, W. O.; Krüger, H.-J. *Angew. Chem., Int. Ed. Engl.* **1996**, *34*, 2671–2674.
- (74) Chow, T. W.; Wong, E. L.; Guo, Z.; Liu, Y.; Huang, J. S.; Che, C. M. *J. Am. Chem. Soc.* **2010**, *132*, 13229–13239.